

We are IntechOpen, the world's leading publisher of Open Access books Built by scientists, for scientists

6,900

Open access books available

186,000

International authors and editors

200M

Downloads

Our authors are among the

154

Countries delivered to

TOP 1%

most cited scientists

12.2%

Contributors from top 500 universities



WEB OF SCIENCE™

Selection of our books indexed in the Book Citation Index
in Web of Science™ Core Collection (BKCI)

Interested in publishing with us?
Contact book.department@intechopen.com

Numbers displayed above are based on latest data collected.
For more information visit www.intechopen.com



Determining the Characteristics of Acoustic Emission in the Fatigue Crack Growth of Aluminum Alloy 2025 for Online Structural Monitoring

Javad Sharifi Ghaderi

Abstract

In the use of metals, due to industrial advances and the application of more dynamic loads, it is necessary to pay more attention to the fatigue issue. Non-destructive inspection methods are used to condition and health monitoring of structures at the time of production and even during the service life of parts. Among non-destructive methods, the acoustic emission method has become a standard and reliable method in recent years. In this project, the characteristics of acoustic emission in the fatigue crack growth of aluminum alloy 2025 for online structural monitoring have been investigated and determined. Acoustic emission tests have been performed in two parts: bending fatigue test with the aim of initiation of fatigue cracks in aluminum alloy 2025 specimens and following tensile tests with the aim of growth of fatigue cracks. The acoustic emission signals and parameters sent by the acoustic emission sensor during both tests were received and recorded by the acoustic emission software. According to the received acoustic emission information, various diagrams are plotted. Analyzing the results from online acoustic emission monitoring showed, the acoustic emission method can be considered as a suitable and reliable technique for detecting crack initiation and crack growth in aluminum alloy 2025.

Keywords: fatigue, bending fatigue test, tensile test, acoustic emission test, aluminum alloy 2025, acoustic emission signal, acoustic emission counts

1. Introduction

1.1 Fatigue failures

Fatigue failure is the most common type of failure because 75 to 90% of material failure in engineering components occurs due to cyclic loading [1]. This type of failure mainly occurs in systems where force or moments is applied continuously but vary in size. Failures that occur under dynamic loading conditions are called fatigue failures. There is no obvious change in the metal structure that fractures due

to fatigue that it can be used as evidence to identify the causes of fatigue failure [1]. With the advance of industry and the increase in the number of machines such as cars, airplanes, compressors, pumps, turbines, etc. that are under repeated load and vibration, fatigue has become more common. The main reason that fatigue failure is dangerous is that it occurs suddenly and invisibly [1]. The beginning of the failure of the part due to fatigue is the initiation of microscopic cracks and then their growth. Crack growth continues until the cross-section of the metal is so small that the stress on it is greater than the ultimate strength of the metal so brittle failure occurs in the specimen. For this reason, failure will be sudden. The fatigue failure surface consists of a smooth area due to friction with the growth of cracks in the section and a rough area that is softly broken in the part when the load is intolerance by the section [2]. **Figure 1** shows fatigue failure of the Bonanza F33 propeller, which is made of aluminum alloy 2025.



Figure 1.
Fatigue failure of bonanza F33 propeller.

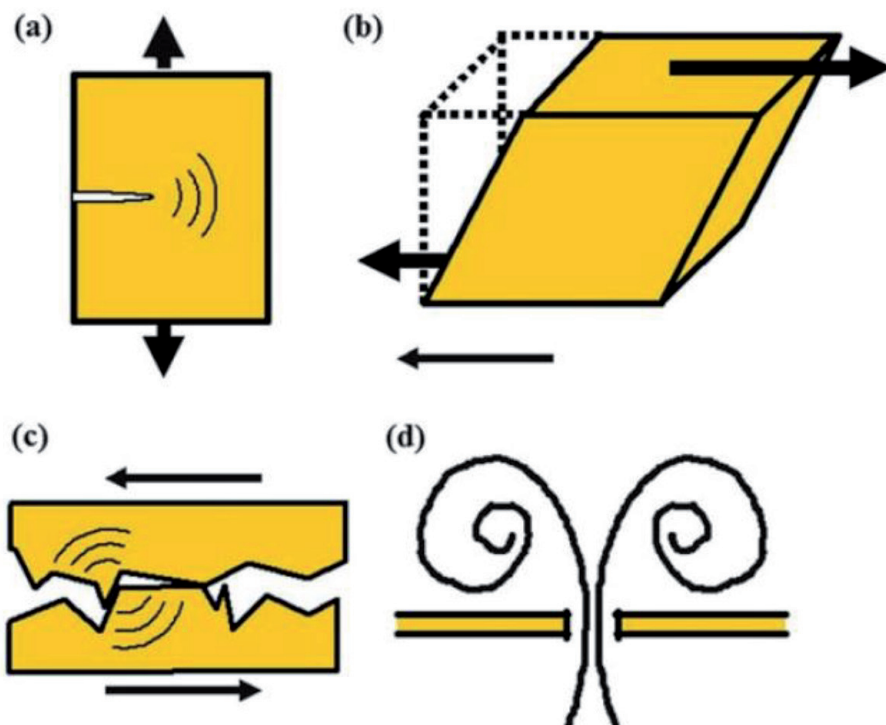


Figure 2.
Example of sources of acoustic emission. (a) Cracking. (b) Deformation and transformation. (c) Slip. (d) Leakage.

1.2 Acoustic emission

Non-destructive testing methods, especially acoustic emission methods, are used to condition monitor of engineering structures [3]. Acoustic emission as a phenomenon can be defined as transient elastic waves caused by internal micro-displacements in the materials of the tested structures. Acoustic emission, as defined by the American Society for Testing and Materials, refers to the class of phenomena whereby transient elastic waves are generated by the rapid release of energy from localized sources within material under stress [4]. Due to its high sensitivity, this method can detect processes such as micro-crack initiation and growth, displacement, failure, slip, leakage, or sediment separation [5]. **Figure 2** shows typical mechanisms that generate acoustic emission waves. The main sources of acoustic emission in metals are plastic deformation and crack growth processes, which are energy-release mechanisms at the scale of crystalline microstructure.

The acoustic emission method has advantages over other non-destructive testing methods, such as the dynamics of this inspection method and the ability to display crack growth online in the structure under load and during service. Other advantages of this method are high speed of testing, accurate location of defects, high efficiency, less sensitivity to the geometry of the part compared to other methods, and detection of very small and micro-scale defects [3].

2. Specimens and experimental equipment

2.1 Aluminum alloy 2025 specimens

According to the structure determination test, the material of the extracted specimen from the propeller blade was determined as aluminum alloy 2025. Due to the limited dimensions of the propeller blade and the impossibility of extracting the specimen with standard dimensions in the standard reference ASTM-E855-08, the dimensions of the test specimen are selected very close to the standard dimensions [6]. Based on this, the length, width, and thickness of the specimen equal to 160 mm, 30 mm, and 4 mm are selected and specimens with these dimensions are extracted. Also, to initiate a crack, a notch with a thickness of 1.5 mm and 1.25 mm width is created parallel to the width of the specimen and at a distance of 27 mm along the length of the part. This notch helps to increase the speed of crack initiation in the specimen. **Figure 3** shows the aluminum alloy 2025 specimen dimensions.

2.2 Bending fatigue machine

In bending fatigue tests with the aim of initiation of cracks from the notch created in the 2025 aluminum specimen, we need a bending fatigue machine. The fatigue machine designed to test aluminum alloy 2025 specimens are mounted on a lathe and receives the moment and force applied to the specimen for fatigue from the machine's engine. The rotational motion created by the motor is converted to linear motion through the crankshaft connected to the drill chuck of the device and the connecting rod. This linear motion is then transmitted to one side of the specimen by a bar. The other side of the sample is fixed with a clamp so that we can see the movement on only one side [7]. **Figure 4** shows the bending fatigue machine. The bending fatigue test is performed in the case of fixed grip loading with a rate of 12 mm per cycle.

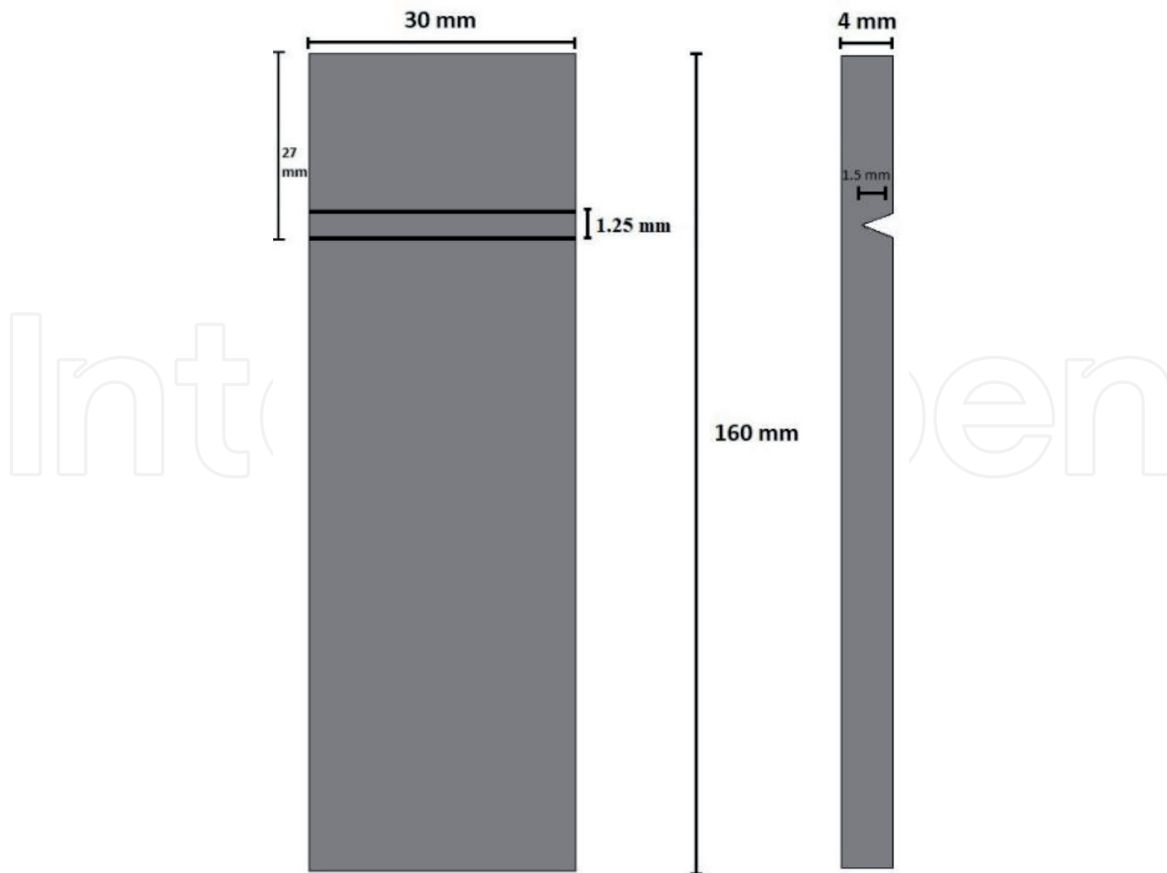


Figure 3.
Schematic and dimension of aluminum alloy 2025 specimen.

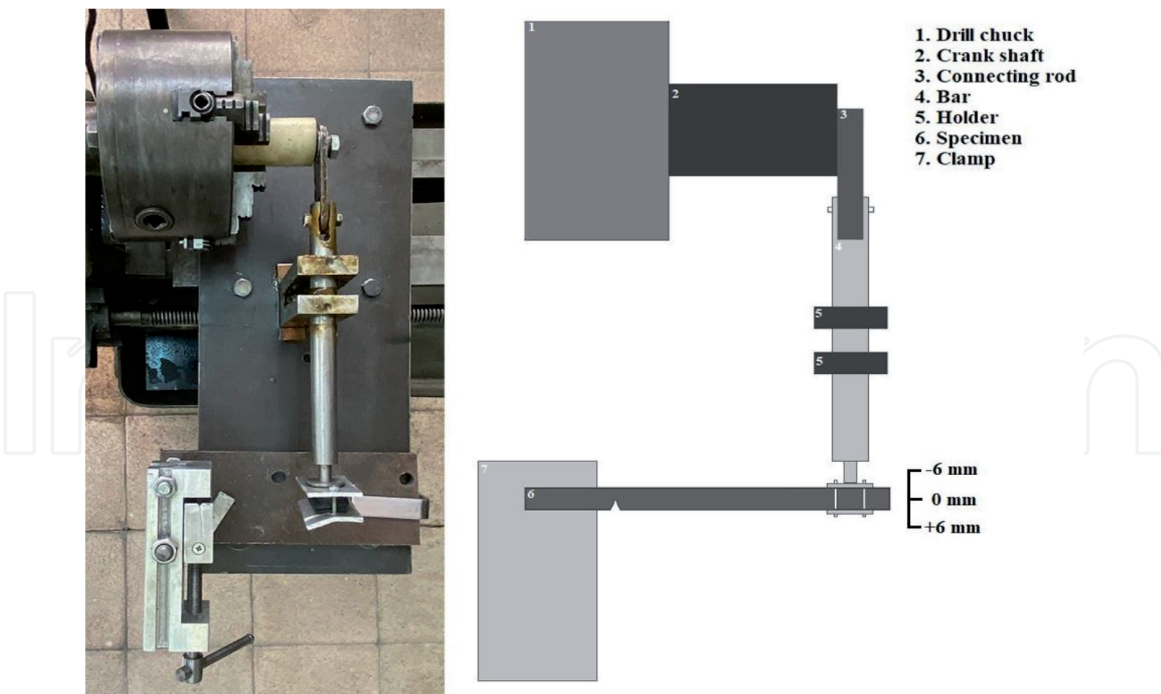


Figure 4.
Schematic and component of bending fatigue machine.

2.3 Tensile machine

In the tensile test, to record the signals emitted from the growth of fatigue cracks in aluminum alloy 2025, we need to grow the initiated cracks in the bending fatigue test by the tensile machine. This device is made by the HIWA company and

has two jaws to connect the two sides of the specimen and a load cell to measure the tensile force. **Figure 5** shows the schematic of tensile machine. Cracked specimens are attached to both jaws of the machine on both sides, and after determining the tensile speed (1 mm/min in this test), the upper jaw of the machine starts to move upwards at the set speed and the initiated crack begins to grow [8].

2.4 Acoustic emission system

This system includes an acoustic emission sensor, a preamplifier, and acoustic emission software. The acoustic emission sensor used in this test is made of Lead-Zirconate with a diameter of 5 mm and a height of 4 mm of broad-band type and is connected to the preamplifier via a cable. The preamplifier has an input that can gain the signal received from the acoustic emission sensor with coefficients of 20, 40, and 60 dB. In this test, a coefficient of 40 dB was used and the output part sends the signal by cable to the computer for processing. The software installed on the computer is called AEwin for PCI-2, which allows us to set the parameters of acoustic emission testing, interpretation, display, and analysis of waveforms, adjust and display and compare several graphs, etc. [9]. **Figure 6** shows the schematic of acoustic emission system. After plotting various diagrams such as acoustic emission

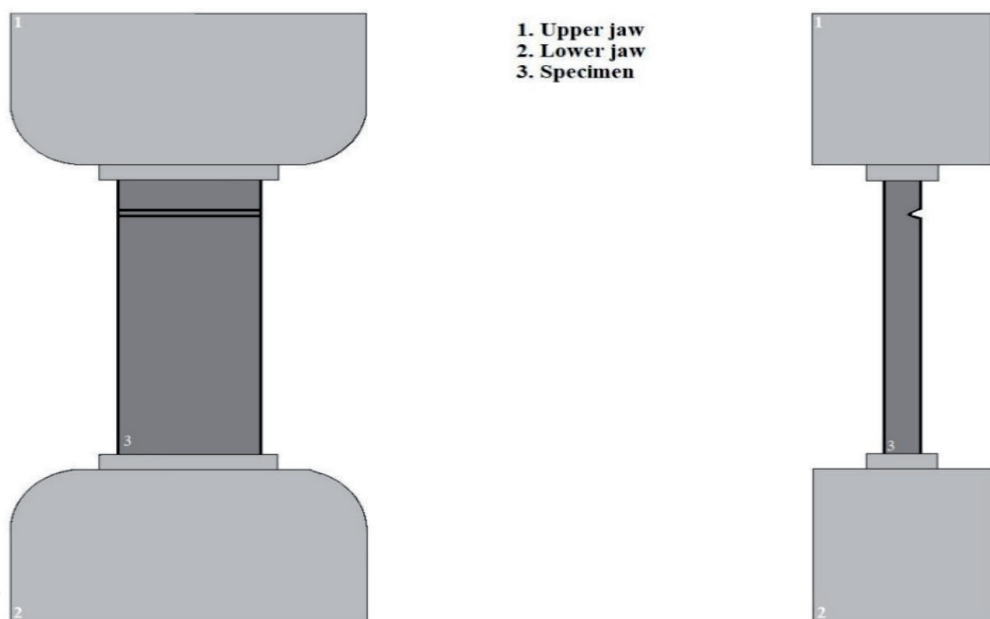


Figure 5.
Schematic and component of tensile machine.

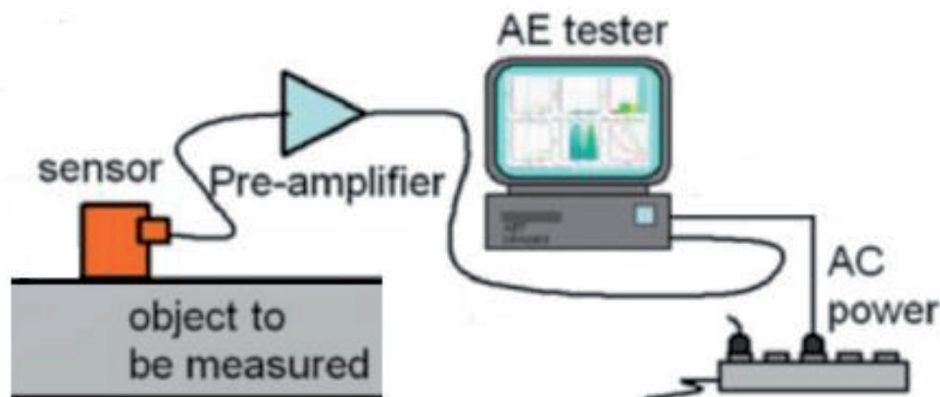


Figure 6.
Schematic of acoustic emission system.

signal amplitude vs. standard cycle diagram and acoustic emission cumulative count vs. standard cycle diagram by the acoustic emission system, and by analyzing the acoustic emission parameters such as signal amplitude, counts, rise time and duration time (In this test, acoustic emission amplitude and count were used), the crack initiation and crack growth can be determined.

The threshold was determined based on ambient noise in the bending fatigue test of 45 dB and in the tensile test of 20 dB, the frequency between 20 kHz to 1 MHz and the sampling rate of 2 MHz per second were determined in acoustic emission software.

3. Overview of experimental results

3.1 Bending fatigue test results (crack initiation)

3.1.1 Acoustic emission signal amplitude versus standard cycle diagram

The first plotted diagram is signal amplitude vs. normalized cycle. This diagram shows the signal amplitude in each standardized cycle. This diagram is important because it determines the recognizability of the signals and is also directly proportional to the magnitude of the event that occurred at the source [3, 10].

After examining the signal amplitude vs. standard cycles for all specimens, it was determined that in each specimen in a different cycle, the signal amplitude starts to increase sharply, then this amount reaches its maximum, and then begins to decrease. The amplitude of the start signal changes from 80–96% of the maximum signal amplitude in the specimens.

This increase in signal amplitude in the diagrams indicates the occurrence of an event within the test specimen. For example, the signal amplitude vs. normalized cycle diagram for specimen NO. 9, which is randomly selected from 9 specimens to explain in detail is shown in **Figure 7**. In the specified part, the signal amplitude in the standardized cycle 15 reaches 52 dB after the increase, then this value increases again until it reaches its maximum value in cycle 18, which is 54 dB, and then it starts to reduce. **Figure 8** shows acoustic emission signal amplitude vs. standard cycle for all 9 specimens.

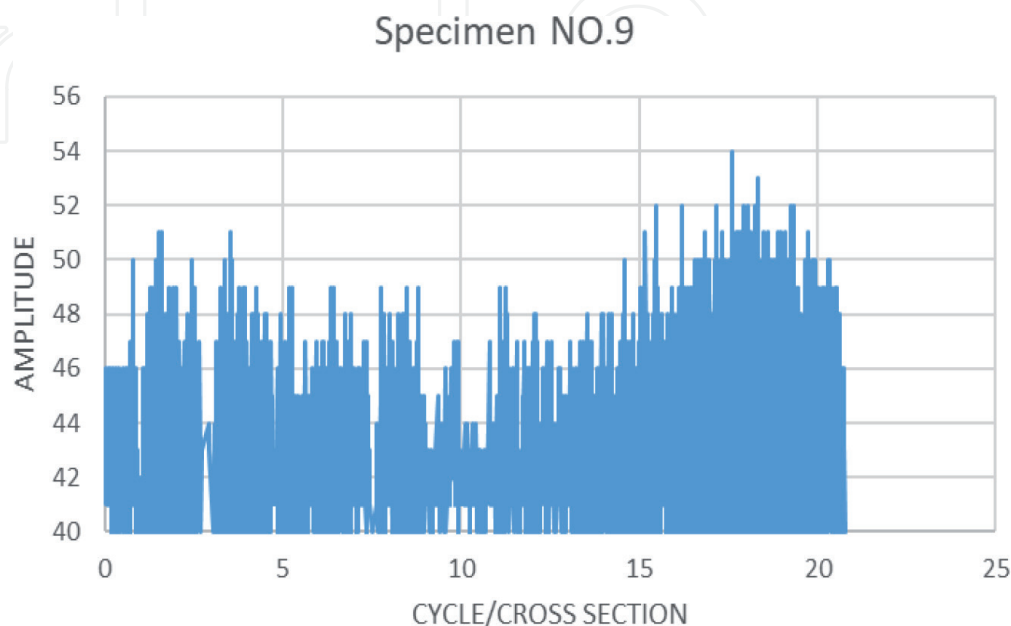


Figure 7.
Acoustic emission signal amplitude vs. standard cycle diagram of specimen NO. 9.

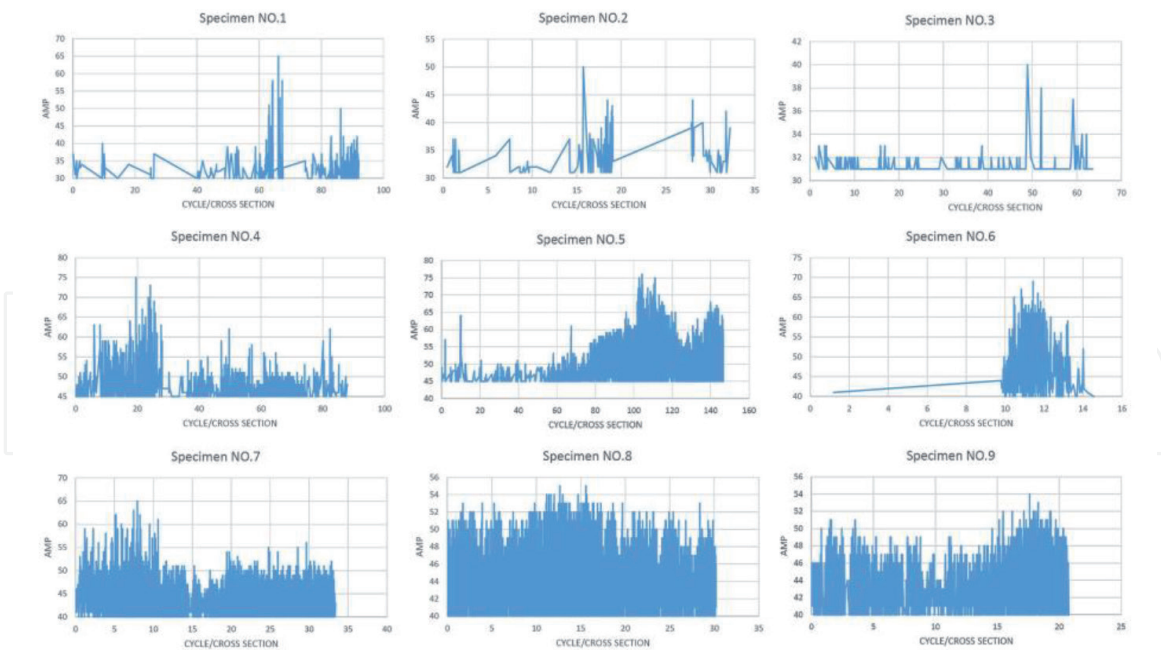


Figure 8.
 Acoustic emission signal amplitude vs. standard cycle diagram for all 9 specimens.

Table 1 shows the maximum signal amplitude and amplitude which signal change start in all 9 specimens.

3.1.2 Acoustic emission cumulative count versus standard cycle diagram

The count is the number of pulses that exceed the specified threshold value [3, 10]. The cumulative count vs. normalized cycle diagram, in each standard cycle, shows the total number of counts of that cycle with previous cycles. The number of counts indicates the internal events of the material [11]. Therefore, where the counts reach their maximum value, the rate of internal events of materials is also at its maximum. After examining the amplitude vs. standard cycle diagram and determining the start cycle of changes in each specimen, to ensure the results are obtained, the cumulative count vs. standard cycle diagram is examined.

To study and analyze changes in cumulative graphs, slope changes in different parts of the graph are used. After examining the slope in different parts of the

Specimen number	Amplitude of start signal changes (dB)	Max. signal amplitude (dB)
NO. 1	52	65
NO. 2	40	50
NO. 3	33	40
NO. 4	63	75
NO. 5	68	76
NO. 6	65	69
NO. 7	62	65
NO. 8	53	55
NO. 9	52	54

Table 1.
 Max. Signal amplitude and amplitude of start signal changes in each specimen.

cumulative count vs. standard cycle diagram, it was determined that before standard cycle NO. 10, an increase in slope is observed in all specimens, which is due to the instability of the conditions at the beginning of the test. After the simultaneous start of the acoustic emission system and the bending fatigue machine, the acoustic emission sensors receive the noise due to the mechanical vibration of the device after starting and display it as an acoustic emission signal which increases the slope in the cumulative counting vs. standard cycle diagram. The slope then continues almost uniformly until the same standard cycle as the amplitude of the signals began to increase, the slope of the cumulative count vs. standard cycle also begins to increase sharply. For example, the acoustic emission cumulative count vs. normalized cycle diagram for specimen NO. 9 is shown in **Figure 9**.

Figure 10 shows the cumulative count vs. standard cycle diagrams for specimens NO. 1 to 9. In diagram of specimen NO. 1, in the standard cycle, approximately 68 to 76 diagrams are in a horizontal line, which is the reason for stopping

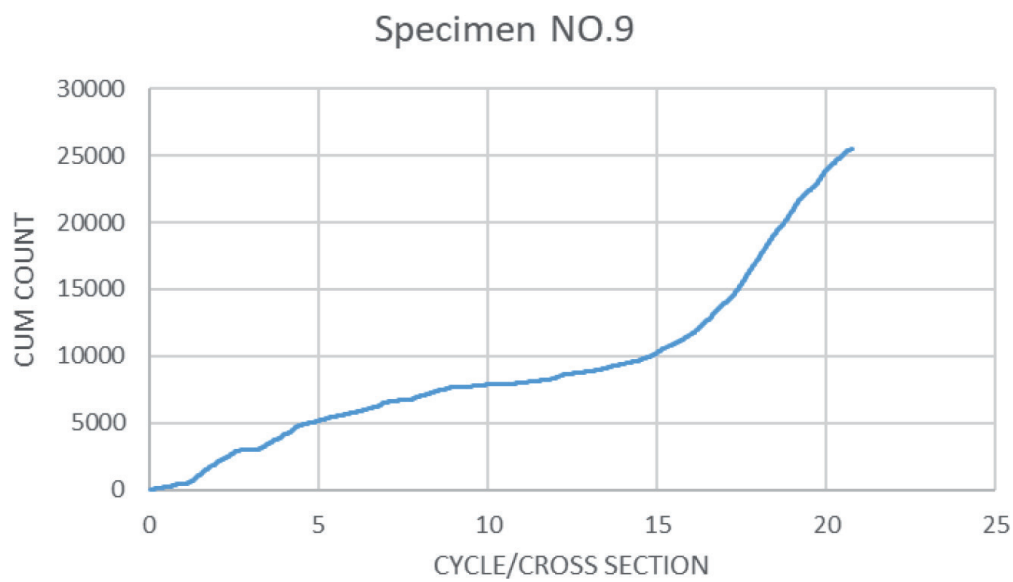


Figure 9.
Acoustic emission cumulative count vs. standard cycle diagram of specimen NO. 9.

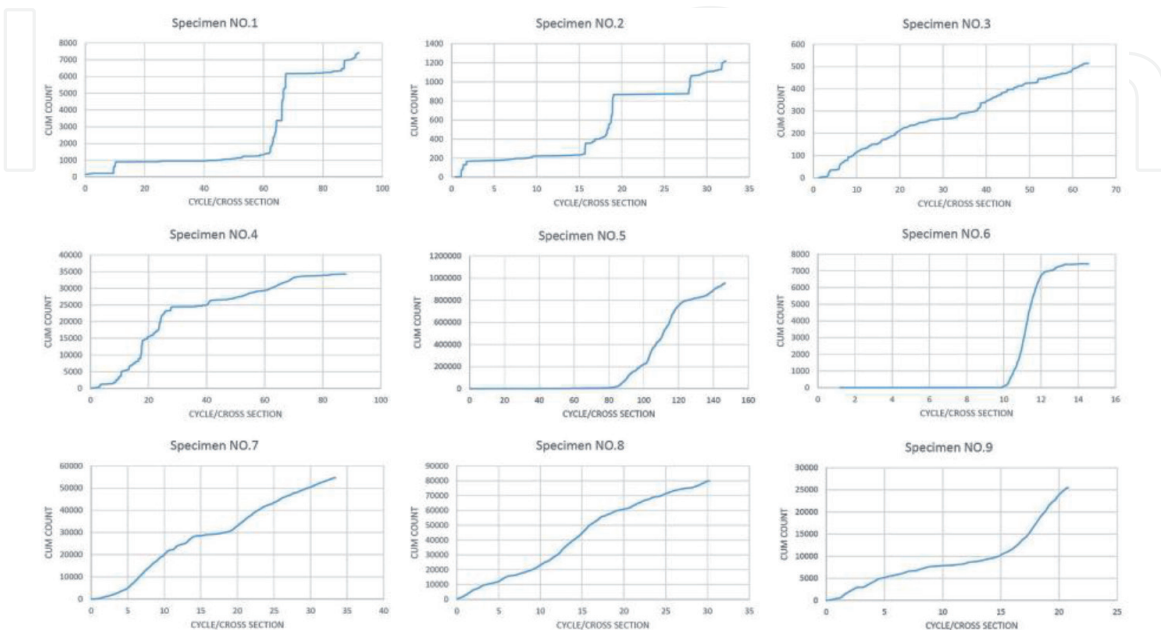


Figure 10.
Acoustic emission cumulative count vs. standard cycle diagram for all 9 specimens.

the test in 30 to 33 minutes. In diagram of specimen NO. 2, this event also occurred in the approximate cycle of 20 to 28, which is from 3 to 4:30 minutes.

For example, in specimen NO. 9, which was also examined in the signal amplitude vs. standard cycle diagram, in standard cycle NO. 15, which is the beginning of changes, it has a cumulative count of 10259, and in standard cycle NO. 20, which is the end of these changes, it has a cumulative count 23893. The slope of the change in the chart is 2870, which is 4 times more than before the start of the experiment when the slope is 703. In all specimens, this sharp increase in slope is noticeable. As mentioned, where the count reaches its maximum value, the rate of the internal events of the material is also at its maximum, in all specimens, the maximum value of the count is in the same range of changes. According to the above, examining the diagrams and the slope of different parts of the diagram, it can be concluded that crack initiation occurs when the slope of the diagram increases sharply. This increase in slope varies from 4 times to 16 times the slope before cracking between the tested specimens.

Table 2 shows maximum acoustic emission count and cycle which signal change start.

For better understand the simultaneity of increasing the signal amplitude and increasing the slope of the cumulative count diagram, the amplitude and cumulative count versus standard cycle diagrams plotted. **Figure 11** shows acoustic emission signal amplitude and cumulative count vs. standard cycle diagram for all 9 specimens.

3.2 Tensile test results (crack growth)

3.2.1 Aluminum alloy 2025 stress: Strain curve

The stress–strain curve is obtained by loading objects at a constant speed and measuring the amount of deformation in the tensile test. In this test, a specimen without any crack is installed on the tensile and is pulled at a speed of 1 mm per second. Using the results of this test, the stress–strain curve is plotted and the yield stress and ultimate stress in aluminum alloy 2025 are obtained. After testing and plotting the stress–strain curve, the ultimate stress level was 381.67 MPa and the yield stress was 275 MPa. The ultimate stress level for aluminum alloy 2025-T3 is 400 MPa in Ref. [12]. **Figure 12** shows stress–strain curve of aluminum alloy 2025 specimen that extracted from propeller blade. The difference between the measured stress and the reference stress is due to the life of the specimen used in the test because as the life of aluminum-containing copper alloy increases, this aluminum becomes brittle.

Specimen number	Cycle number of start signal changes	Max. acoustic emission count
NO. 1	64	523
NO. 2	15	111
NO. 3	39	13
NO. 4	8	436
NO. 5	102	396
NO. 6	11	70
NO. 7	6	48
NO. 8	11	67
NO. 9	15	39

Table 2.
 Max. Acoustic emission count and cycle number of start signal changes in each specimen.

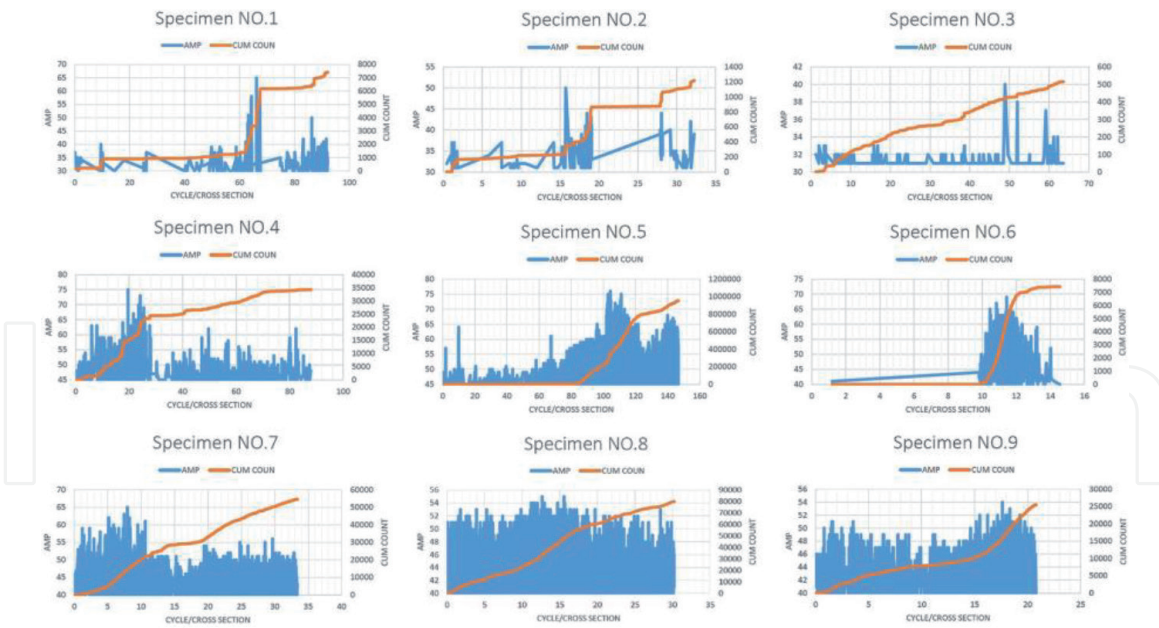


Figure 11. Acoustic emission signal amplitude and cumulative count vs. standard cycle diagram for all 9 specimens.

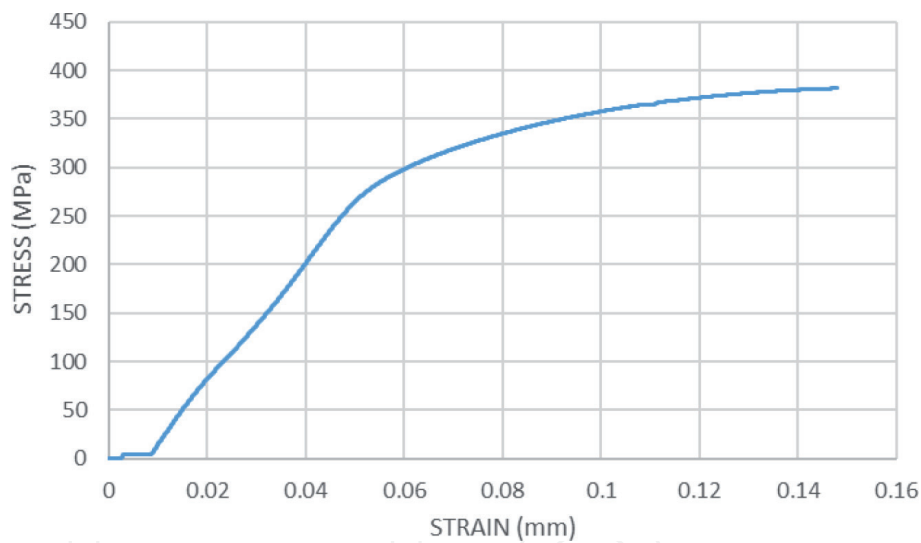


Figure 12. Stress–strain curve of aluminum alloy 2025.

3.2.2 Acoustic emission count and stress versus time diagram

After performing the bending fatigue test and recording and analyzing the acoustic emission parameters due to crack initiation, it is necessary to subject the cracked specimens in the bending fatigue test to the tensile load to determine the parameters and characteristics of acoustic emission in fatigue crack growth. After performing the tensile test on 5 of the cracked specimens in the bending fatigue test, it is time to plot the count and stress vs. time diagram. This diagram shows the rate count and stress at each point in time of the test. Because all sources of additional signals and noise are blocked, the received signals are related to the acoustic emission activities inside the specimen. In general, these acoustic emission activities may be the result of plastic deformation or the growth of fatigue cracks created in the specimens. Because the test specimen is aluminum alloy 2025 with long life and brittle material and there is no sign of deformation in the specimen,

the signals received by the sensor cannot be the plastic deformation signals so these signals are due to the growth of fatigue cracks.

After examining the count and stress vs. time diagram, it was found that with increasing stress, which is obtained by dividing the tensile force on the cross-section of the specimen, the count also increases. As mentioned in the previous paragraph, this increase in the count is related to the growth of cracks in the aluminum specimen. According to the **Figure 13**, which shows the count and stress vs. time diagram for specimen NO. 1, which is randomly selected from 5 specimens to explain in detail, the count does not increase continuously and the increase in count occurs after increasing the slope of the stress diagram.

Figure 14 shows the count and stress vs. time diagrams for all 9 specimens. As can be seen from the figure, in all specimens, the count increases sharply at the end of the test time, which indicates the highest crack growth activity during the test or an increase in crack growth rate with increasing force.

The highest increase of count for specimen NO. 1 occurred from 160 seconds to 167 seconds, where the highest rate of crack growth was observed. **Figure 15** shows the condition of the crack in 3 different times. Figure (a) shows the crack condition before the tensile test, when in the bending fatigue test the test is stopped immediately after observing the crack initiation. Figure (b) is after increasing the count



Figure 13.
 Acoustic emission count, and stress vs. time diagram of specimen NO. 1.

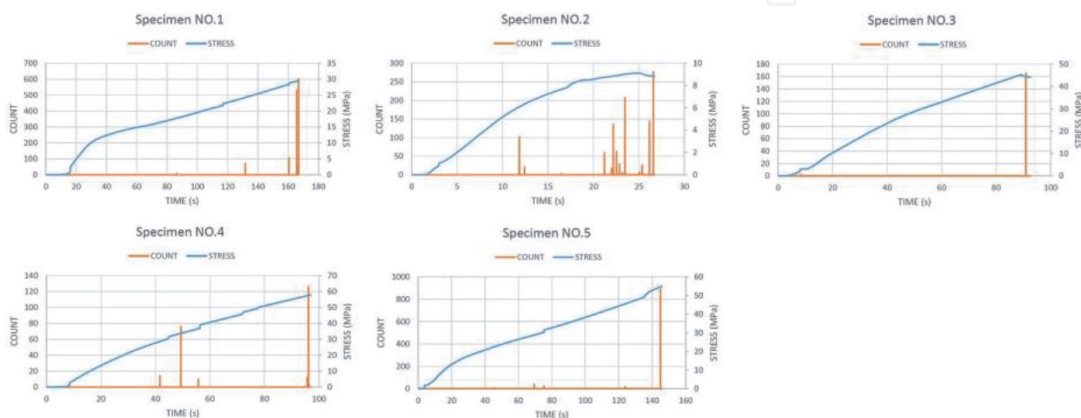


Figure 14.
 Acoustic emission count, and stress vs. time diagram for all 9 specimens.

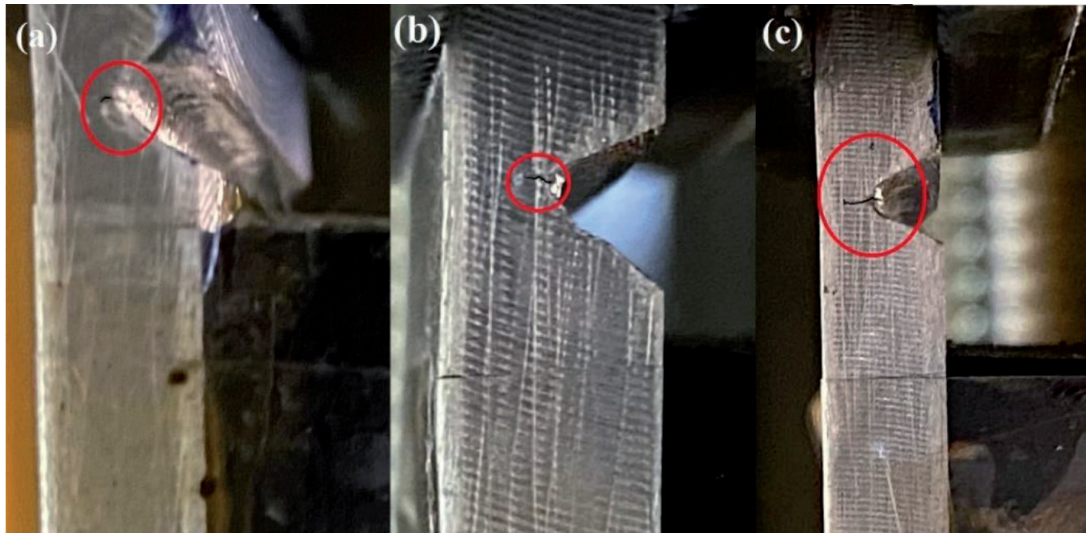


Figure 15.
Crack condition during specimen NO. 1 test (a) before tensile test (b) in 160 second (c) in 167 second.

at 160 seconds, where the count increases to 106 and the cumulative count to 189. Figure (c) also refers to a time of 167 seconds, where a sharp increase in the count, first at 165 seconds at 530 and then at 166 seconds at 602.

As the crack growth and the count diagram show, as time goes on and the stress and force increase, the count rate increase too, so the internal activity of the material and the crack growth increase, so that the maximum crack growth rate at the end of the test of each specimen.

4. Conclusion

Bending fatigue test and tensile test were performed on aluminum alloy 2025 specimens and acoustic emission characteristics were recorded and examined in each of the tests. One of the purposes of this project was to investigate the feasibility of the acoustic emission method in detecting the initiation and growth of fatigue crack growth in Bonanza f33 propellers. The analysis of this method was performed by examining specimens of propeller with aluminum alloy 2025.

The first part of the tests, bending fatigue test with the aim of crack initiation and recording the acoustic emission signals emitted from the aluminum alloy 2025 specimen. After reviewing and analyzing the amplitude vs. standard cycle diagram and cumulative count vs. standard cycle diagram, it was determined that the sharp increase of the signal amplitude to the maximum signal and the sharp increase of the slope of the cumulative count occurs in the same standard cycle. This time can be attributed to crack initiation. The slope of the count vs. standard cycle at the start of crack initiation increases more than four times this slope from the start of the test.

The second part of the tests, the tensile test was performed to grow the cracks created in the previous stage and record the acoustic emission signals caused by the growth of fatigue cracks in aluminum alloy 2025. To determine the condition of the specimens and plot a stress–strain curve, first the tensile test was performed on a specimen of aluminum alloy 2025 without a notch. After plotting the stress–strain curve, the yield stress was equal to 275 MPa and the ultimate stress was equal to 381.67 MPa.

Analysis of the parameters and diagrams of count and stress vs. time in the tensile test shows an increase in the count with increasing force. The highest rate of crack growth occurs at the end of each test, because the highest number of counts, which indicates the internal events of a specimen, is observed at the end

of the test. An increase in the number of counts in the loading phase indicates the growth of cracks.

As a final conclusion, despite the brittle material of aluminum alloy 2025, the acoustic emission method is a reliable, accurate, and high-efficiency method to identify the initiation and growth of fatigue crack in this aluminum alloy.

IntechOpen

IntechOpen

Author details

Javad Sharifi Ghaderi
Shahid Sattari University of Aeronautical Engineering, Tehran, Iran

*Address all correspondence to: javadsharifighaderi@gmail.com

IntechOpen

© 2021 The Author(s). Licensee IntechOpen. This chapter is distributed under the terms of the Creative Commons Attribution License (<http://creativecommons.org/licenses/by/3.0>), which permits unrestricted use, distribution, and reproduction in any medium, provided the original work is properly cited. 

References

- [1] Chawla K. K, Meyers M.A. Mechanical behavior of materials. 2nd ed. Cambridge university press; 2008. 1132 p. DOI:10.1017/CBO9780511810947
- [2] Kushan M. C, Diltemiz S. F, Sackesen I, Engineering failure analysis: Failure analysis of an aircraft propeller. FEBS Letters. 2007;513:1693-1700. DOI:10.1016/j.engfailanal.2006.11.069
- [3] Mizutani Y. Practical acoustic emission testing. 2nd ed. Springer; 2006. 1132 p. DOI:10.1007/9784431550723
- [4] Nondestructive evaluation and test. ASTM hand book. 9th ed.; 1994. Vol 17. 1132 p. DOI:10.1520/STP624-EB
- [5] Peng-jing Zhao, Yan-dond Sun, Jing-pin Jiao, Gang Fang, Engineering fracture mechanics: Correlation between acoustic emission detection and microstructural characterization for damage evolution. Vol. 230, May 2020. DOI:10.1016/j.engfracmech.2020.106967
- [6] Bending Test Methods for Bend Testing of Metallic Flat Materials for Spring Application Involving. ASTM; 2013. 1132 p. DOI:10.1520/E0855-08R13
- [7] Pritam. V. Kulkarni, P. J. Sawant, V. V. Kulkarni, Materials today: Design and development of plane bending fatigue testing machine for composite material. 2018, 11563-11568. DOI:10.1016/j.matpr.2018.02.124
- [8] Standard test methods for tension testing of metallic materials E8/E8M. An American National Standard; 2013. DOI:10.1520/E0008_E0008M-16A
- [9] Zinoviy Nazarchuk, Valentyn Skalskyi, Oleh Serhiyenko. Acoustic emission methodology and application. 1st ed. Springer; 2017. DOI:10.1007/978-319-49350-3
- [10] Prosser W.H. The Propagation Characteristics of the Plate Modes of Acoustic Emission Waves in Thin Aluminum Plates and Graphite/Epoxy Composite Plate and Tubes [Thesis]. Maryland: John Hopkins University; 1991.
- [11] Blanchette Y, Dickson J. I, Bassim M. N, Engineering fracture mechanics: Acoustic emission behavior crack growth of 7075-T651 Al alloy. FEBS Letters. 1986;513:647-656. DOI: 10.1016/0013-7944(86)90240-7
- [12] AZoM. Aluminum 2025 alloy (UNSA92025) [Internet]. 2013. Available from: www.azom.com/article.aspx?ArticleD=8718 [Accessed: 2013-05-17]